Computational Mechanics (1990) 6, 129–142

Computational Mechanics

Vibration isolation using open or filled trenches

Part 2: 3-D homogeneous soil

B. Dasgupta
Department of Civil and Mineral Engineering, University of Minnesota, Minneapolis, MN 55455, USA

D. E. Beskos
Department of Civil Engineering, University of Patras, Patras 26110, Greece

I. G. Vardoulakis
Department of Civil and Mineral Engineering, University of Minnesota, Minneapolis, MN 55455, USA

Abstract. The isolation of structures from ground transmitted waves by open and infilled trenches in a three-dimensional context is numerically studied. The soil medium is assumed to be elastic or viscoelastic, homogeneous and isotropic. Waves generated by the harmonic motion of a surface rigid machine foundation are considered in this work. The formulation and solution of the problem is accomplished by the boundary element method in the frequency domain. The infinite space fundamental solution is used requiring discretization of the trench surface, the soil-foundation interface and some portion of the free soil surface. The proposed methodology is first tested for accuracy by solving three characteristic wave propagation problems with known solutions and then applied to several vibration isolation problems involving open and concrete infilled trenches. Three-dimensional graphic displays of the surface displacement pattern around the trenches are also presented.

1 Introduction

Screening of waves generated by a surface disturbance for structural vibration isolation is usually achieved by constructing a barrier, e.g., an open or infilled trench, which through diffraction of elastic waves results in vibration amplitude reduction (Richart et al. 1970).

A comprehensive account of the literature on the experimental, analytical and numerical analysis of vibration isolation and associated wave diffraction problems can be found in a recent publication by Beskos et al. (1986). That publication as well as another one by the same authors (Beskos et al. 1985), presented a numerical treatment of these problems by the Boundary Element Method (BEM) under two-dimensional (2-D) conditions (plane strain). The present work represents an extension of the methodology of Beskos et al. (1985, 1986) to three-dimensional (3-D) vibration isolation problems and provides numerical results for a number of practical cases. Among the few published analytical works on three-dimensional elastic wave diffraction problems one can mention those of Knopoff (1959a, b), Pao and Mow (1963, 1971) and Jain and Kanwal (1978) who studied diffraction of P and S waves by spherical cavities and inclusions and Lee (1982), and Lee and Trifunac (1982) who analysed diffraction of plane waves (P, SV and SH) by a hemispherical canyon and rigid foundation, respectively, in the elastic half space for an arbitrary angle of wave incidence. It is apparent that analytic treatment of 3-D elastic wave diffraction problems is confined to very simple geometries and that realistic problems involving complex geometry, such as vibration isolation ones, can only be solved numerically.

The BEM is ideally suited for elastic wave diffraction problems involving infinite or semi-infinite 3-D domains and, as it has been demonstrated in various places and especially in a recent review article by Beskos (1987) and the very recent book of Manolis and Beskos (1988), it is more advantageous than either the Finite Element Method (FEM) or the Finite Difference Method (FDM). Quite a number of accurate and efficient algorithms for 3-D elastodynamic analysis by the direct BEM in the frequency or time domain has recently appeared in the literature. One can mention, for example, those of Dominguez (1978a, b), Dominguez and Alarcón (1981), Ottenstreuer and Schmid (1981), Ottenstreuer (1982), Huh and Schmid (1984), Rizzo et al. (1985a–c), Rezayat et al. (1986), Niwa and Hirose (1985, 1986), Kobayashi and Mori (1986), Kobayashi et al. (1986), Kitahara and Nakagawa (1985), Nakagawa and Kitahara (1986), Kitahara et al. (1987), Karabalis

and Mohammadi (1986), Gaitanaros and Karabalis (1986) and Ahmad and Manolis (1987), in the frequency domain and Karabalis and Beskos (1984, 1985, 1986), Manolis (1984), Banerjee et al. (1986) and Ahmad and Banerjee (1988) in the time domain. General and special review type of articles dealing with both the frequency and the time domain direct BEM and its applications emphasizing 3-D aspects have also appeared very recently in the literature. One can mention here, e.g., those of Banerjee and Ahmad (1985), Banerjee et al. (1987), Kobayashi (1987), Karabalis and Beskos (1987a, b), Dominguez and Abascal (1987), Tassoulas (1989) and especially Beskos (1987). A comparison study between frequency and time domain BEM approaches in 3-D soil-structure interaction has been recently reported by Mohammadi and Karabalis (1986).

The present work employs the frequency domain direct BEM for the solution of both passive and active vibration isolation problems in a 3-D context. The general harmonic motion of a rigid foundation generates waves which are reduced in amplitude by means of open or infilled trenches protecting nearby structures. The geometry of the foundation or the trench can be arbitrary but the applications are restricted here to rectangular foundations and rectangular trenches which are usually preferred in practice. The soil medium is assumed to be a linear elastic or viscoelastic, homogeneous and isotropic half-space. The methodology employed in this work is just an extension to 3-D of the methodology utilized by Beskos et al. (1985, 1986) for the same problem under conditions of plane strain. Thus, constant quadrilateral boundary elements and the infinite space fundamental elastodynamic solution are employed in this work. Constant elements have been chosen because of their simplicity and their low memory requirements for such a large order problem which involves a foundation, a half-space and a trench treated all together in a 3-D context. It is apparent that constant elements are, in general, not as accurate as higher order ones, e.g., quadratic elements for 3-D wave diffraction problems, especially when detailed information is needed nearfield and/or there are stress concentrations (e.g., Rizzo et al. 1985a; Banerjee et al. 1987). However, in the special case of vibration isolation problems, the free surface response away from the trench is of more interest than the deformation of the trench itself or the stress concentrations around it and thus, constant elements can produce results of acceptable accuracy for this type of problems. This was verified by solving three representative wave propagation problems with known solutions. The infinite space fundamental solution, on the other hand, was also chosen because of its simplicity over the very complicated half-space fundamental solution (e.g., Kobayashi and Nishimura 1980; Luco and Apsel 1983; Apsel and Luco 1983). Use of the former solution requires a discretization of a finite portion of the free half-space surface, which is not required by the latter solution. However, in vibration isolation problems, information is needed on the free half-space surface and hence a discretization of this surface is anyhow required.

The work presented in this paper, is part of the doctoral dissertation of the first author (Dasgupta 1987) which can be consulted for more details. Some preliminary results of this work have also been reported in Dasgupta et al. (1986). Following a presentation of the formulation and solution procedure, a number of characteristic vibration isolation cases are treated in subsequent sections by the proposed methodology and their results are presented both in conventional two-dimensional plots and in colored three-dimensional graphics, which provide an impressive picture of the wave diffraction phenomenon associated with vibration isolation.

2 General BEM formulation of 3-D elastodynamics

The present formulation of 3-D linear elastodynamic problems by the direct frequency domain BEM is just a 3-D extension of the 2-D formulation in Beskos et al. (1986). Thus the frequency domain equations of motion for a 3-D homogeneous, isotropic and linear elastic body B with boundary S and zero body forces are of the form (Eringen and Suhubi 1975)

$$(c_1^2 - c_2^2)\bar{u}_{i,ij} + c_2^2\bar{u}_{j,ii} + \omega^2\bar{u}_j = 0; \quad i, j = 1, 2, 3, \tag{1}$$

where $\bar{u}_i = \bar{u}_i(\underset{\sim}{x}, \omega)$ are the displacement amplitudes, the point $\underset{\sim}{x}$ has Cartesian coordinates x_1, x_2 and x_3, ω is the circular frequency, commas indicate spatial differentiation and summation over

repeated indices is assumed. The c_1 and c_2 in (1) are propagation velocities of compressional (P) and shear (S) waves, respectively, which are given in terms of Lamé's elastic constants λ and μ and the mass density ρ of the material by

$$c_1^2 = (\lambda + 2\mu)/\rho, \quad c_2^2 = \mu/\rho \tag{2}$$

The constitutive equation is of the form

$$\bar{\sigma}_{ij} = \rho[(c_1^2 - 2c_2^2)\bar{u}_{k,k}\delta_{ij} + c_2^2(\bar{u}_{i,j} + \bar{u}_{j,i})], \tag{3}$$

where $\bar{\sigma}_{ij} = \bar{\sigma}_{ij}(\underset{\sim}{x}, \omega)$ are the stress amplitudes and δ_{ij} is Kronecker's delta. Initial conditions are assumed to be zero, while the mixed type boundary conditions take the form

$$\bar{\sigma}_{ij} n_j = \bar{t}_{i0}(\underset{\sim}{x}, \omega); \quad \underset{\sim}{x} \in S_\sigma, \tag{4}$$

$$\bar{u}_i = \bar{u}_{i0}(\underset{\sim}{x}, \omega); \quad \underset{\sim}{x} \in S_u, \tag{5}$$

where n_j stands for the outward unit normal vector component at the boundary $S = S_\sigma + S_u$, and $\bar{t}_{i0}$ and $\bar{u}_{i0}$ represent prescribed boundary values for the traction and displacement vectors, respectively.

In order to solve the system of Eqs. (1–5) by the BEM, use is made of the boundary integral equation (Eringen and Suhubi 1975)

$$\tfrac{1}{2}u_j(P) = -\int_S \bar{u}_i(Q)\bar{T}_{ji}(Q,P)dS(Q) + \int_S \bar{t}_i(Q)\bar{U}_{ji}(Q,P)dS(Q). \tag{6}$$

In Eq. (6) $\bar{U}_{ij}$ and $\bar{T}_{ij}$ are the singular influence tensors (fundamental solution or Green's functions) for the infinite space which are given explicitly by (Eringen and Suhubi 1975)

$$\bar{U}_{ij} = \frac{1}{4\pi\rho\omega^2 r^3}\{\delta_{ij}[(k_2 r)^2 e_2 + D] + C r_{,i} r_{,j}\}, \tag{7}$$

$$\bar{T}_{ij} = \frac{1}{4\pi\rho\omega^2 r^4}\left\{\lambda e_1 (k_1 r)^2 \Gamma_1 r_{,j} n_i + \mu e_2 (k_2 r)^2 \Gamma_2 \left(\delta_{ij}\frac{\partial r}{\partial n} + r_{,i} n_j\right)\right.$$
$$\left. + 2\mu\left[C\left(\delta_{ij}\frac{\partial r}{\partial n} + r_{,j} n_{,i} + r_{,i} n_{,j}\right) + F r_{,i} r_{,j}\frac{\partial r}{\partial n}\right]\right\}, \tag{8}$$

where

$$\begin{aligned} &k_\alpha = \omega/c_\alpha, && e_\alpha = e^{ik_\alpha r}, \quad \alpha = 1,2, \\ &D = \Gamma_2 e_2 - \Gamma_1 e_1; && \Gamma_\alpha = -1 + ik_\alpha r, \\ &C = \Omega_2 e_2 - \Omega_1 e_1; && \Omega_\alpha = 3 - 3ik_\alpha r - k_\alpha^2 r^2, \\ &F = H_1 e_1 - H_2 e_2; && H_\alpha = 15 - 15ik_\alpha r - 6k_\alpha^2 r^2 + ik_\alpha^3 r^3. \end{aligned} \tag{9}$$

In the above, r is the distance between two boundary points P and Q and $i = \sqrt{-1}$ (when not subscripted).

The solution of Eq. (6) is accomplished numerically. For this purpose the boundary S of the body B is discretized into a number of N, in general unequal in size, boundary elements (flat triangular or quadrilateral) over which the stress and displacement vectors are assumed to be constant. Equation (6) can thus reduce in its discretized form to the matrix equation

$$[\overline{\mathbf{GT}}]\{\bar{\mathbf{u}}\} - [\overline{\mathbf{GU}}]\{\bar{\mathbf{t}}\} = \mathbf{0}, \tag{10}$$

where $\{\bar{\mathbf{u}}\}$ and $\{\bar{\mathbf{t}}\}$ are the displacement and traction vectors, respectively, in the frequency domain and $[\overline{\mathbf{GT}}]$ and $[\overline{\mathbf{GU}}]$ are square influence matrices consisting of elemental surface integrals with integrands the tensors $\bar{T}_{ij}$ and $\bar{U}_{ij}$, respectively. When $Q \neq P$, i.e., $r \neq 0$, these integrals are regular and integration is accomplished by using standard Gauss quadrature. When $Q \to P$, i.e., $r \to 0$, these integrals become singular due to the $0(1/r)$ and $0(1/r^2)$ singularities of the tensors $\bar{U}_{ij}$ and $\bar{T}_{ij}$, respectively, and they have to be computed analytically. Explicit analytic expressions for these singular integrations can be found in Dasgupta (1987). The presence of the terms $e^{ik_\alpha r}$ in

the fundamental tensors make the integrands increasingly oscillatory for high frequencies ω. Thus, for high values of ω, the numerical integration scheme over a given boundary element must account for these oscillations. A 3×3 Gauss quadrature scheme was found to be adequate for the chosen frequency of oscillation and the adopted size of the elements. For more information on this subject one can consult Rizzo et al. (1985a) and Rezayat et al. (1986).

The above formulation assumes linear elastic material behavior. However, it is also valid for linear viscoelastic material behavior provided that the elastic moduli λ and μ are replaced by the complex moduli

$$\lambda^* = \lambda(1 + i\beta), \quad \mu^* = \mu(1 + i\beta), \tag{11}$$

where the damping factor β is usually taken to be independent of frequency (hysteretic material). Use of damping in the formulation, as it is the case with the present paper, makes the problem of the fictitious eigenfrequencies (Rizzo et al. 1985a, b) to disappear.

3 Matrix formulation of 3-D wave diffraction problems

This section deals with the development of the BEM matrix formulation of various 3-D wave diffraction problems including vibration isolation ones. In the following, bars over harmonic amplitudes are omitted for simplicity.

3.1 Scattering of incident waves

Consider an incident time harmonic plane wave propagating in the half-space which is diffracted by surface irregularities such as trenches of arbitrary shape. Figure 1 shows a rectangular trench on the surface of the half-space. The total boundary S consists of the free soil surface S_f and the trench surface S_t. Formulation of the wave scattering problem in terms of the scattered field is accomplished by writing the boundary integral Eq. (10) in the form

$$\begin{bmatrix} [\mathbf{GT}]^g_{11} & [\mathbf{GT}]^g_{12} \\ [\mathbf{GT}]^g_{21} & [\mathbf{GT}]^g_{22} \end{bmatrix} \begin{Bmatrix} \{\mathbf{u}^s\}_f \\ \{\mathbf{u}^s\}_t \end{Bmatrix} = \begin{bmatrix} [\mathbf{GU}]^g_{11} & [\mathbf{GU}]^g_{12} \\ [\mathbf{GU}]^g_{21} & [\mathbf{GU}]^g_{22} \end{bmatrix} \begin{Bmatrix} \{\mathbf{t}^s\}_f \\ \{\mathbf{t}^s\}_t \end{Bmatrix}, \tag{12}$$

where the superscripts g and s stand for "ground" and "scattered", respectively, and the subscripts f and t correspond to quantities on S_f and S_t. The total field of displacements $\{\mathbf{u}\}$ and tractions $\{\mathbf{t}\}$ can be written as

$$\{\mathbf{u}\} = \{\mathbf{u}^i\} + \{\mathbf{u}^s\}; \qquad \{\mathbf{t}\} = \{\mathbf{t}^i\} + \{\mathbf{t}^s\} \quad \text{on} \quad S = S_f + S_t \tag{13, 14}$$

The boundary conditions of the problem read

$$\{\mathbf{t}\} = \{\mathbf{0}\} \quad \text{on} \quad S = S_f + S_t \tag{15}$$

Substitution of Eq. (15) in (14) and partitioning yield

$$\begin{Bmatrix} \{\mathbf{t}^i\}_f \\ \{\mathbf{t}^i\}_t \end{Bmatrix} + \begin{Bmatrix} \{\mathbf{t}^s\}_f \\ \{\mathbf{t}^s\}_t \end{Bmatrix} = \begin{Bmatrix} \{\mathbf{0}\} \\ \{\mathbf{0}\} \end{Bmatrix} \tag{16}$$

For the incident field, the free surface of the half-space is stress-free, i.e.,

$$\{\mathbf{t}^i\}_f = \{\mathbf{0}\}. \tag{17}$$

Combination of Eqs. (16) and (17) results in

$$\{\mathbf{t}^s\}_f = \{\mathbf{0}\} \quad \text{on } S_f; \quad \{\mathbf{t}^s\}_t = -\{\mathbf{t}^i\}_t \quad \text{on } S_t \tag{18, 19}$$

Thus, the problem consists of solving Eq. (12) for $\{\mathbf{u}^s\}_f$ and $\{\mathbf{u}^s\}_t$ subject to the boundary conditions (18) and (19). Knowledge of the vectors $\{\mathbf{u}^i\}$ and $\{\mathbf{u}^s\}$ allows one to determine $\{\mathbf{u}\}$ from (13) along the boundary S.

3.2 *Vibration isolation of foundation*

In this section, vibration isolation of rigid, massive, rectangular, machine foundations in perfect bonding with the soil subjected to time harmonic forces, as shown in Fig. 1, are studied with the aid of the proposed methodology. The amplitude reduction of the waves generated by the motion of the foundation is accomplished by open or infilled trenches. This method takes into account all the waves generated by the vibrating footing, not just Rayleigh waves, and it treats the foundation-trench system as a whole. Furthermore, it is not restricted to rigid foundations and after some modifications can be applied to flexible, embedded foundations with or without mass under relaxed or nonrelaxed boundary conditions. In the following, the case of the foundation-infilled trench isolation system is considered. The simpler case of the foundation-open trench isolation system can be obtained as a special case.

Consider the foundation-infilled trench isolation system of Fig. 1, which consists of three parts, the soil half-space, the infilled trench and the rigid foundation. These are related to each other through the compatibility and equilibrium equations at their interfaces. Use of the boundary integral Eq. (10) for the half-space and the infill medium results in the matrix equations

$$\begin{bmatrix} [\mathbf{GT}]^g_{11} & [\mathbf{GT}]^g_{12} & [\mathbf{GT}]^g_{13} \\ [\mathbf{GT}]^g_{21} & [\mathbf{GT}]^g_{22} & [\mathbf{GT}]^g_{23} \\ [\mathbf{GT}]^g_{31} & [\mathbf{GT}]^g_{32} & [\mathbf{GT}]^g_{33} \end{bmatrix} \begin{Bmatrix} \{\mathbf{u}\}_r \\ \{\mathbf{u}\}_f \\ \{\mathbf{u}\}_t \end{Bmatrix} = \begin{bmatrix} [\mathbf{GU}]^g_{11} & [\mathbf{GU}]^g_{12} & [\mathbf{GU}]^g_{13} \\ [\mathbf{GU}]^g_{21} & [\mathbf{GU}]^g_{22} & [\mathbf{GU}]^g_{23} \\ [\mathbf{GU}]^g_{31} & [\mathbf{GU}]^g_{32} & [\mathbf{GU}]^g_{33} \end{bmatrix} \begin{Bmatrix} \{\mathbf{t}\}_r \\ \{\mathbf{t}\}_f \\ \{\mathbf{t}\}_t \end{Bmatrix}, \tag{20}$$

$$\begin{bmatrix} [\mathbf{GT}]^c_{11} & [\mathbf{GT}]^c_{12} \\ [\mathbf{GT}]^c_{21} & [\mathbf{GT}]^c_{22} \end{bmatrix} \begin{Bmatrix} \{\mathbf{u}_c\}_t \\ \{\mathbf{u}_c\}_o \end{Bmatrix} = \begin{bmatrix} [\mathbf{GU}]^c_{11} & [\mathbf{GU}]^c_{12} \\ [\mathbf{GU}]^c_{21} & [\mathbf{GU}]^c_{22} \end{bmatrix} \begin{Bmatrix} \{\mathbf{t}_c\}_t \\ \{\mathbf{t}_c\}_o \end{Bmatrix}, \tag{21}$$

respectively, where the scripts g, f, r, t, c and o refer to quantities for the ground (soil), the free soil surface, the soil-foundation interface, the trench surface, the infill (concrete) and the top surface of the infill, respectively.

The compatibility of displacements at the interface of the rigid foundation with the soil can be expressed in matrix form as

$$\{\mathbf{u}\}_r = [\mathbf{S}]\,\{\mathbf{e}\}, \tag{22}$$

where $[\mathbf{S}]$ is a $3N \times 3$ matrix connecting the displacements of the N interface elements with those of the vector

$$\{\mathbf{e}\} = \{\Delta_1, \Delta_2, \Delta_3\}, \tag{23}$$

with Δ_i $(i = 1, 2, 3)$ being the displacement of the foundation center along the x_i axis. The rigid foundation is subjected to the externally applied load

$$\{\mathbf{p}\} = [p_1\ p_2\ p_3] \tag{24}$$

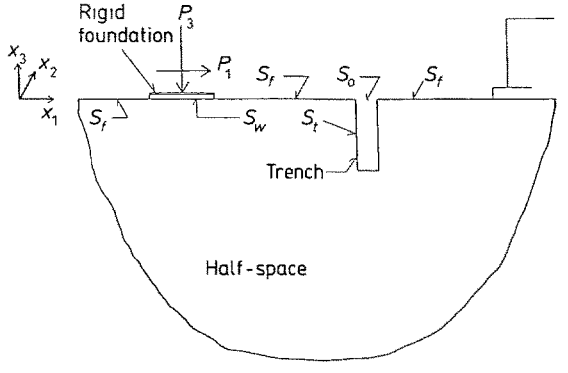

Fig. 1. Vibration isolation of machine foundation by infilled trench

which can be expressed in terms of the contact stresses using equilibrium of forces and take the form

$$p_i = -m\omega^2\Delta_i + \sum_{k=1}^{N} A_k \sigma_{3i}^k, \tag{25}$$

where m is the mass of the foundation, A_k represents the area of the k-th foundation element and $\sigma_{3i}^k = t_i^k$ are the interface tractions of the k-th foundation element. Equation (25) can be written for all the N contact area elements as

$$\{\mathbf{p}\} = [\mathbf{J}]\{\mathbf{e}\} + [\mathbf{H}]\{\mathbf{t}\}_r, \tag{26}$$

where $[\mathbf{J}]$ and $[\mathbf{H}]$ are 3×3 and $3 \times 3N$ matrices.

The compatibility and equilibirum conditions at the soil–infill interface read

$$\{\mathbf{t}_c\}_t = -\{\mathbf{t}\}_t; \quad \{\mathbf{u}_c\}_t = \{\mathbf{u}\}_t, \tag{27}$$

respectively. The soil free surface S_f and the top infill surface S_o are free of tractions, i.e.,

$$\{\mathbf{t}\}_f = \{\mathbf{0}\}, \quad \{\mathbf{t}_c\}_o = \{\mathbf{0}\} \tag{28}$$

Rewriting Eqs. (20) and (21) in compact form as

$$\{\mathbf{t}\} = [\mathbf{G}]\{\mathbf{u}\}, \quad \{\mathbf{t}_c\} = [\mathbf{F}]\{\mathbf{u}_c\}, \tag{29}$$

with

$$[\mathbf{G}] = [\mathbf{GU}^g]^{-1}[\mathbf{GT}^g], \quad [\mathbf{F}] = [\mathbf{GU}^c]^{-1}[\mathbf{GT}^c], \tag{30}$$

enables one to expand Eqs. (20) and (21) as

$$\begin{aligned}
\{\mathbf{t}\}_r &= [\mathbf{G}_{11}]\{\mathbf{u}\}_r + [\mathbf{G}_{12}]\{\mathbf{u}\}_f + [\mathbf{G}_{13}]\{\mathbf{u}\}_t,\\
\{\mathbf{t}\}_f &= [\mathbf{G}_{21}]\{\mathbf{u}\}_r + [\mathbf{G}_{22}]\{\mathbf{u}\}_f + [\mathbf{G}_{23}]\{\mathbf{u}\}_t,\\
\{\mathbf{t}\}_t &= [\mathbf{G}_{31}]\{\mathbf{u}\}_r + [\mathbf{G}_{32}]\{\mathbf{u}\}_f + [\mathbf{G}_{33}]\{\mathbf{u}\}_t,\\
\{\mathbf{t}_c\}_t &= [\mathbf{F}_{11}]\{\mathbf{u}_c\}_t + [\mathbf{F}_{12}]\{\mathbf{u}_c\}_o,\\
\{\mathbf{t}_c\}_o &= [\mathbf{F}_{21}]\{\mathbf{u}_c\}_t + [\mathbf{F}_{22}]\{\mathbf{u}_c\}_o
\end{aligned} \tag{31}$$

Combining Eqs. (31) with Eqs. (22), (26), (27) and (28) one finally receives the matrix equation

$$\begin{Bmatrix} \{\mathbf{p}\} \\ \{\mathbf{0}\} \\ \{\mathbf{0}\} \end{Bmatrix} = \begin{bmatrix} [\hat{\mathbf{G}}_{11}] & [\hat{\mathbf{G}}_{12}] & [\hat{\mathbf{G}}_{13}] \\ [\hat{\mathbf{G}}_{21}] & [\mathbf{G}_{22}] & [\mathbf{G}_{23}] \\ [\hat{\mathbf{G}}_{31}] & [\hat{\mathbf{G}}_{32}] & [\hat{\mathbf{G}}_{33}] \end{bmatrix} \begin{Bmatrix} \{\mathbf{e}\} \\ \{\mathbf{u}\}_f \\ \{\mathbf{u}\}_t \end{Bmatrix}, \tag{32}$$

where

$$\begin{aligned}
&[\hat{\mathbf{G}}_{11}] = [\mathbf{H}][\mathbf{G}_{11}][\mathbf{S}] - [\mathbf{J}], \quad [\hat{\mathbf{G}}_{12}] = [\mathbf{H}][\mathbf{G}_{12}],\\
&[\hat{\mathbf{G}}_{13}] = [\mathbf{H}][\mathbf{G}_{13}], \quad [\hat{\mathbf{G}}_{21}] = [\mathbf{G}_{21}][\mathbf{S}],\\
&[\hat{\mathbf{G}}_{31}] = [\mathbf{F}_{22}][\mathbf{G}_{31}][\mathbf{S}], \quad [\hat{\mathbf{G}}_{32}] = [\mathbf{F}_{22}][\mathbf{G}_{32}],\\
&[\hat{\mathbf{G}}_{33}] = [\mathbf{F}_{22}][\mathbf{G}_{33}] + [\mathbf{F}_{22}][\mathbf{F}_{11}] - [\mathbf{F}_{12}][\mathbf{F}_{21}].
\end{aligned} \tag{33}$$

Equation (32) can now be easily solved for the displacement vectors $\{\mathbf{e}\}$, $\{\mathbf{u}\}_f$ and $\{\mathbf{u}\}_t$.

4 Numerical examples

In this section two groups of numerical examples are presented. The first group serves to check the accuracy and effectiveness of the proposed constant BEM. The second group deals with several practical vibration isolation problems where the wave barrier effectiveness is the main object of study.

4.1 *Validation of the formulation*

Example 1: Consider a spherical cavity of radius a in the infinite elastic space, radiating waves into the elastic medium due to a uniform harmonic pressure of unit amplitude applied on its surface. The proposed BEM is used to determine the radial displacement u on the surface of the cavity. The employed discretization combining triangular and quadrilateral flat boundary elements covers only the 1/8th of the cavity surface due to the spherical symmetry of the problem. The numerical solution for the normalized frequency $n_1 = a\omega/\pi c_1 = 0.2$ exhibits a 9.14% error with 49 and a 6.6% error with 81 elements relative to the analytic solution $u = -(1/a^2) + (i\omega/c_1 a)$ (Achenbach 1973).

Example 2: Consider the vertical vibration of a rigid, massless square foundation perfectly bonded to the surface of an elastic half-space caused by a harmonic, vertical point force applied at its center. The force-displacement relationship is described by the vertical compliance $C_{vv} = Gbu_3/P_3$ (Wong and Luco 1976), where G is the shear modulus, b is the half side of the foundation and u_3 and P_3 are the amplitudes of the vertical displacement and load, respectively. Figure 2 depicts C_{vv} versus $a_0 = \omega b/c_2$ for an elastic half-space with Poisson's ratio $\nu = 1/3$ and material damping $\beta = 0.01\%$. The proposed BEM results, using 49 constant elements, compare very well with the numerical solutions of Wong and Luco (1976) using 64 constant elements and Rizzo et al. (1985a) using 16 quadratic elements. Table 1 provides the compliance error of the proposed BEM relative to the most accurate one of Rizzo et al. (1985a) for $a_0 = 0.5768$ and three different discretizations. It is apparent that a 25-element discretization with a maximum error of only 1.5% is an acceptable one and for this reason this discretization is adopted in the vibration isolation problems of this section.

Example 3: The surface displacements resulting from the diffraction of a vertically incident plane P-wave by a semi-spherical cavity on the surface of the half-space are determined by the proposed BEM. One quarter of this symmetric problem was analysed by using triangular and quadrilateral flat boundary elements covering the cavity as well as a portion of the half-space free surface around the cavity. The normalized amplitudes of vertical and horizontal displacements on the surface of the half-space for $n_1 = \omega R/\pi c_1 = 0.25$, with R being the canyon radius, are shown in Fig. 3. A Poisson's ratio $\nu = 0.25$ and a 144 element discretization were used in the computations. In the same figure the results obtained by the boundary collocation method of Sánchez-Sesma with 50 to 70 points are also plotted for comparison. The results obtained by the two methods show a satisfactory agreement only for points away from the canyon.

In the above three examples, the basic aspects of wave propagation analysis have been addressed using a constant boundary element methodology. Good results were obtained in the first example, where the harmonic pressure applied on the surface of the cavity was uniform. Excellent results were obtained for the rigid foundation compliance problem in the second example, where the stress is applied on the half-space in an average sense. In the diffraction of the P-wave problem, better results were obtained on the surface of the half-space than on the surface of the canyon. In conclusion, constant boundary elements, characterized by simplicity and low computational cost, can be satisfactorily applied to the present vibration isolation problems where, the external load is applied through the foundation, the discretized surfaces are flat and the surface displacements are of more interest than the deformation of the trench wall.

Table 1. Compliance of rigid foundation for different discretizations

	C_{vv} (Real)			C_{vv} (Imaginary)		
Number of elements	Present method	Rizzo et al. (1985a)	Error %	Present method	Rizzo et al. (1985a)	Error %
3 × 3	0.1278		7.48	0.0654		0.879
5 × 5	0.1207	0.1189	1.5	0.0645	0.0648	−0.509
7 × 7	0.1176		−1.09	0.0641		−1.126

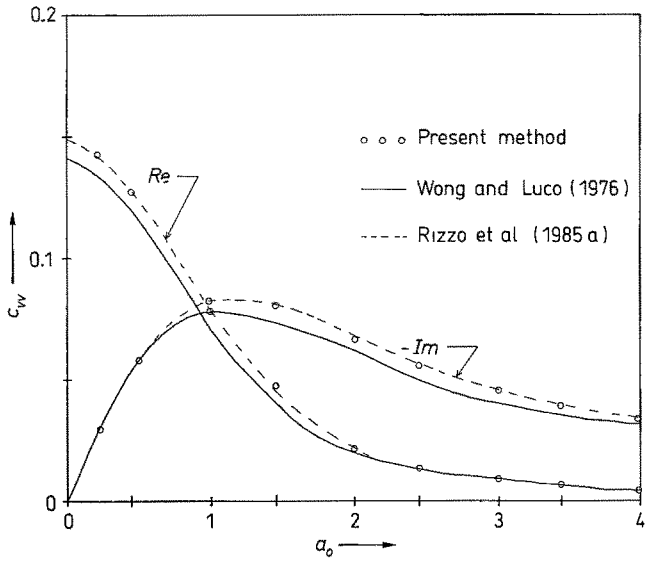

2

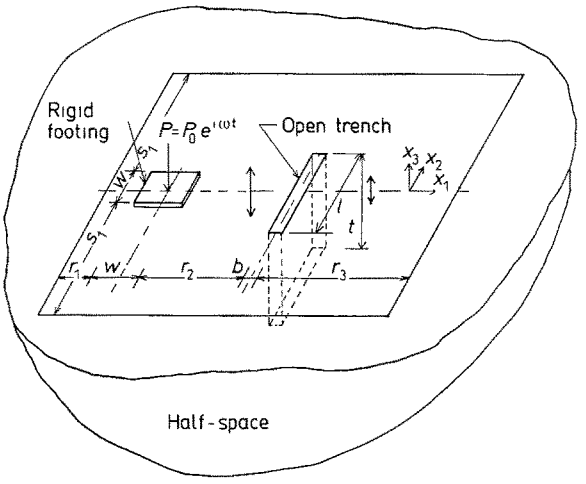

4

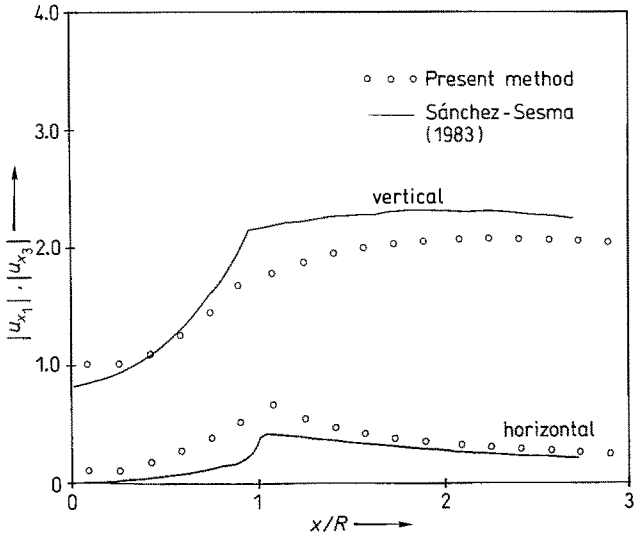

3

3

Figs. 2–4. **2** Vertical compliance for a perfectly bonded square rigid foundation. **3** Surface amplitude of vertical and horizontal displacements for normalized frequency $n_1 = 0.25$. **4** Schematic diagram for the vibration isolation system with rigid foundation and open trench

4.2 Vibration isolation problems

The effectiveness of an open or an infilled trench as a barrier to ground-transmitted waves produced by the vertical motion of a rigid foundation is studied in the following examples. Both passive and active vibration isolation cases are considered. Figure 4 shows a schematic diagram of a representative foundation-trench dynamic system and its geometry.

A 3-D analysis provides a more realistic picture of the wave isolation problem than a 2-D plane strain analysis. In the latter case where the foundation and the trench are infinitely long in the x_2 direction, the wave energy is restricted to propagate in the x_1 and x_3 directions and waves are diffracted by the depth of the trench (Beskos et al. 1986). In the former case, however, the foundation and the trench are of finite size and the wave energy can radiate in all three orthogonal directions. In this case, the waves are diffracted by the depth of the trench and also the trench wall along the x_2 direction. Thus one can nicely observe the regions of reduction and amplification of waves on the surface of the half-space. The screening effectiveness of the trench is determined by evaluation of the amplitude reduction factor A_{RD} defined as the average normalized vertical surface amplitude

behind the trench and given as

$$A_{RD} = \frac{1}{\Delta} \int A(\delta) d\delta, \tag{3}$$

where Δ is the area of the region behind the trench enclosed by the semicircular area with a radius $l/2$ (one-half of the length of the trench) and $A(\delta)$ is the ratio of the vertical amplitude with the trench to that without it. It should be noted that A_{RD} is different from A_R, the amplitude reduction factor used in the 2-D case and calculated over a line behind the trench (Beskos et al. 1986).

In the following examples, certain dimensions of the problem are kept the same for the purpose of comparison. All dimensions are normalized with respect to L_R (5 m), the wave length of the Rayleigh wave. The material properties of the soil medium are given in Table 2. The magnitude of the applied force P_0 in 1 KN and its operational frequency is 50 HZ. The mass of the foundation is neglected, following a 2-D study in Dasgupta (1987) where it was found that the mass of the foundation does not significantly affect isolation of surface waves.

Example 1: Consider the single open trench case described by Fig. 4 with $T = t/L_R = 0.5$, $B = b/L_R = 0.1$, $W = w/L_R = 0.5$, $L = l/L_R = 2.0$, $R_1 = r_1/L_R = 0.2$, $R_2 = r_2/L_R = 1.0$, $R_3 = r_3/L_R = 1.05$, and $S_1 = s_1/L_R = 1.7$. This is a passive vibration isolation case. Due to the symmetry of the problem about the x_1 axis, only one-half of the surface was taken into consideration for the analysis. For this problem and all subsequent problems, the surface was descretized into square elements of size $L_R/10$ and rectangular elements were used along the trench width, with the longest side not greater than $L_R/10$. The surface of the half-space and the surface of the trench were discretized into 588 elements, as shown in Fig. 5, which also depicts the vertical displacement amplitude pattern of the surface of the half-space caused by the diffraction of waves by the trench. The maximum displacement is under the foundation. A natural color spectrum for displacements ranging from high values in red to low values in blue is used in this figure.

Displacement amplification and reduction in various regions are well understood from the normalized vertical displacement, $\bar{V}$, i.e., the ratio of the displacement in the presence of the trench over that without the trench. The normalized displacement pattern can be represented by the 2-D colored contour diagram shown in Fig. 6. In this figure, the color fringes have been designed with fewer colors, to highlight the regions of low and high displacement density behind and in front of the trench, respectively. The area in light red before the trench is the region where $\bar{V}$ is higher than 2.0. The light blue area represents values of $\bar{V}$ less than 0.5, while the dark blue area represents values between 0.5 and 2.0. The green area is the transition zone from the dark blue to the light red, and signifies values lower than 2.0. The open trench creates a magnification of amplitude in front and near the end of the trench and reduction behind the trench, a phenomenon also observed

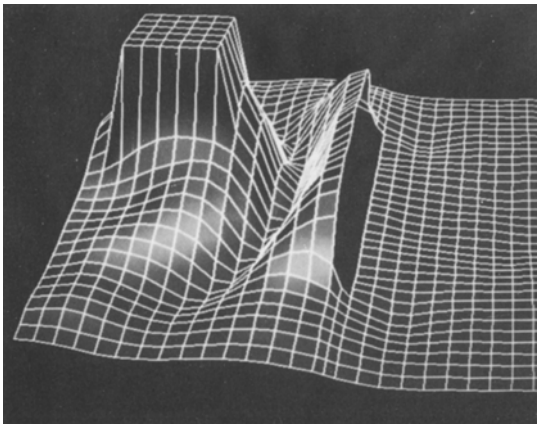

5

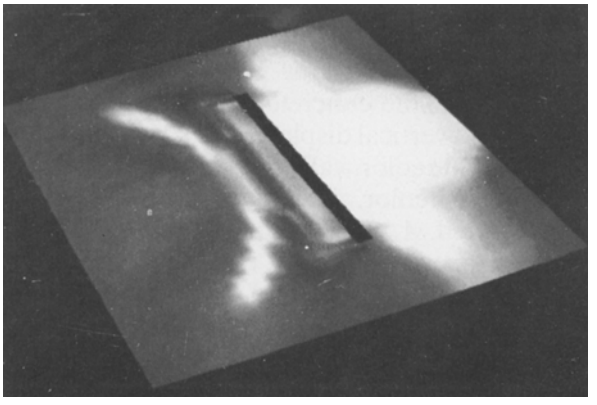

6

Figs. 5 and 6. **5** Vertical displacement amplitude of the surface of half-space; open trench. **6** Contour diagram of the normalized vertical surface amplitude; open trench

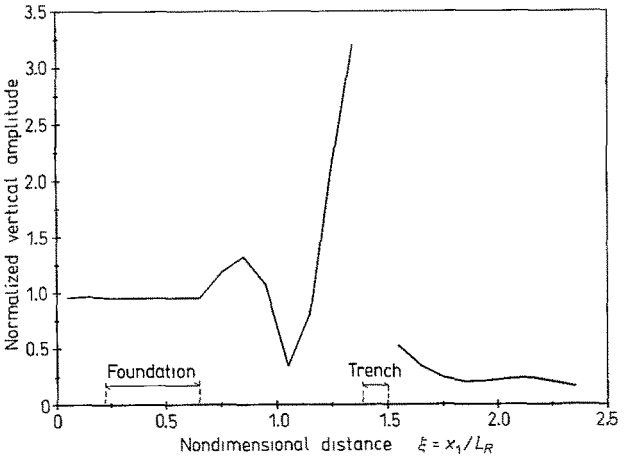

7

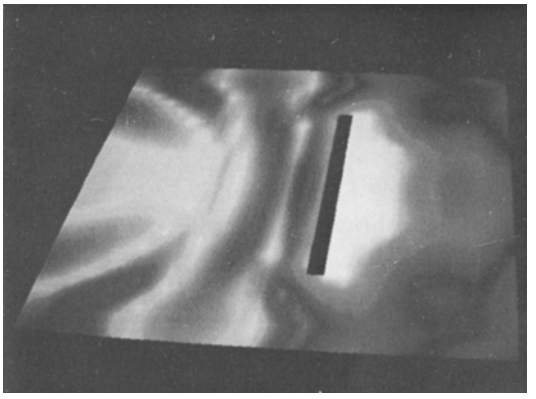

8

Figs. 7 and 8. 7 Normalized surface displacement along the line of symmetry for single open trench. **8** Contour diagram of the normalized vertical surface amplitude, infilled trench

Table 2. Material properties of the half-space medium

Shear modulus	$G_s = 132\,\text{M Pa}$
Poisson's ratio	$\nu_s = 0.25$
Specific weight	$\rho_s = 17.5\,\text{kN/m}^3$
Damping coefficient	$\beta_s = 6\%$
Rayleigh wave velocity	$c_R = 250\,\text{m/sec}$

Table 3. Material properties of the infill medium

Shear modulus	$G_c = 34.29\,G_s$
Poisson's ratio	$\nu_c = \nu_s$
Specific weight	$\rho_c = 1.37\,\rho_s$
Damping coefficient	$\beta_c = 5.0\,\beta_s$
Velocity of Rayleigh wave	$c_R^c = 5.0\,c_R^s$

experimentally by Richart et al. (1970). Figure 7 shows the normalized amplitude of the vertical displacement $\bar{V}$ along the line of symmetry, $\xi = x_1/L_R$. This figure shows magnification in front of the trench and maximum reduction at some distance behind the trench. A similar observation is reported by Richart et al. (1970) on the basis of experimental studies. The amplitude reduction factor A_R calculated along the x_1 axis on the basis of Fig. 7 is 0.26. This compares well with $A_R = 0.29$ for the 2-D analysis, obtained from Fig. 12 of Beskos et al. (1986). This comparison also proves that the 2-D analysis gives a good estimate of vibration isolation effect along the center line of the symmetrical 3-D problem. But when it comes to understanding the screening efficiency of the trench over a region, one should perform a 3-D study. A_{RD} for the open trench is 0.312. The computational time on the Cray 2 computer of the University of Minnesota for this open trench case was about 24 mins.

Example 2: Consider the previous case with the trench being filled with concrete. The material properties of the concrete wall are given in Table 2. Figure 8 depicts the contour diagram of normalized vertical displacements $\bar{V}$, with the light blue color representing values of $\bar{V}$ less than 0.3; the dark blue color, values between 0.9 and 1.0; the light red color, values between 0.9 and 1.0; and the dark red color, values greater than 1.0. The green is the transition color between dark blue and light red. A_{RD} for this problem is 0.258, i.e., A_{RD} for the infilled trench has a much lower value than the one for the open trench. Figure 9 shows the normalized vertical displacement pattern along the line of symmetry, which exhibits considerable differences from the open trench case pattern of Fig. 7. The computational time for this problem was about 31 mins.

Example 3: Consider the active vibration case of Fig. 10 where the open trench surrounds the rigid foundation. The depth of the trench is $T = t/L_R = 0.5$, while the rest of the dimensions are shown in Fig. 10. The foundation load is the same as before and, because of symmetry, one quarter of the region is included in the analysis. The surface of the half-space and the open trench

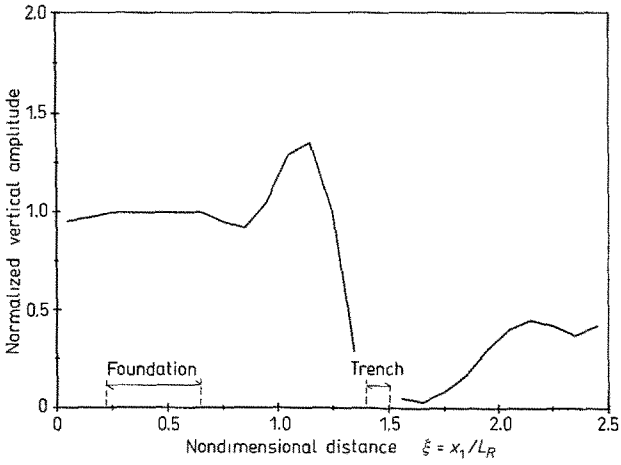

Fig. 9. Normalized surface displacement along the line of symmetry for infilled trench

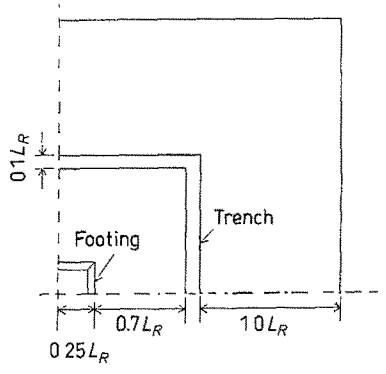

10

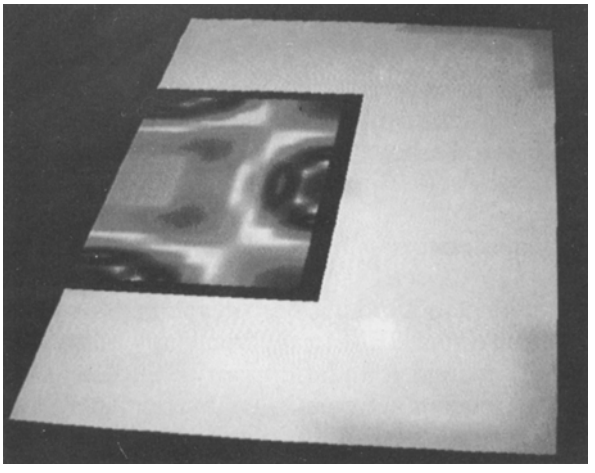

11

Figs. 10 and 11. **10** Dimensions of the vibration isolation problem with open trench enclosing the foundation. **11** Contour diagram of the normalized vertical surface amplitude; enclosed open trench

is discretized into 620 elements. The colored contours of the normalized vertical displacement are shown in Fig. 11 where the light blue color represents values of $\bar{V}$ less than 0.6; the dark blue, values between 0.6 and 3.0; and the red, values greater than 3.0. The maximum $\bar{V}$ on the surface near the edge of the trench is 5.33, much higher than the one for the open trench having a value of 3.5. This increase is caused by reflections from side trenches which are absent in the single open trench problem. The displacements in the region outside the trench have been reduced effectively, as can be seen from the light blue region. The computational time for this problem was about 33 mins.

Example 4: Consider the passive vibration isolation accomplished by three open trenches as shown in Fig. 12. Sometimes it may be desirable to build several small trenches instead of one long trench, because of several site or geological restrictions. Two trenches of length 0.4 L_R are symmetrically placed on either end of a long trench which has a length of 1.3 L_R, as shown in Fig. 12. All the trenches have a depth of $T = t/L_R = 0.5\ L_R$. The foundation is vibrating under an oscillating vertical load with the same characteristics as before. The discretization of one-half of the surface for this symmetric problem involves 608 elements. The displacement pattern, with red to blue color fringes, is shown in Fig. 13. All three open trenches reflect waves, as indicated by the displacement on the edge of the trenches. The A_{RD} for this problem, over the same area

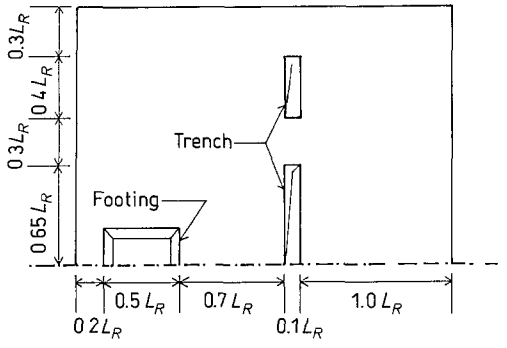

12

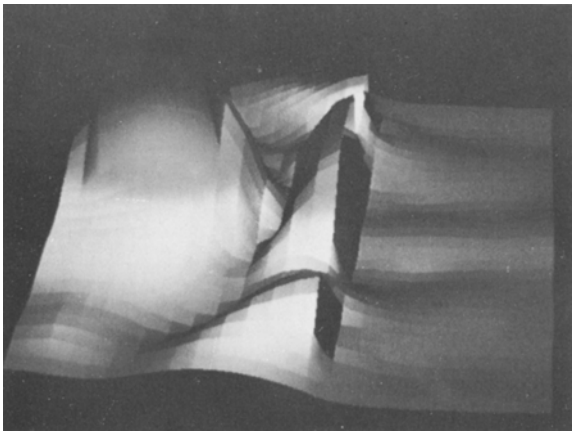

13

Figs. 12 and 13. **12** Dimensions of the vibration isolation problem with three open trenches. **13** Vertical displacement amplitude of the surface of half-space; multiple open trench

as for the single open trench, is 0.415. The A_{RD} is higher than for the single open trench because of the refraction of waves through the region between the trenches. The computational time required was about 26 mins.

5 Conclusions

A numerical method has been developed to solve vibration isolation problems in three dimensions, using the direct BEM in the frequency domain. Thus isolation of waves generated by a vertically oscillating rigid foundation can be successfully studied for various configurations of open and infilled trenches acting as wave barriers in a passive or active fashion. Three-dimensional colored graphics have been used to enhance the visual effects of the surface deformation for a number of selected representative examples.

In this work constant boundary elements have been used for simplicity and low computational cost in view of the very large size of the problem. However, constant elements are not characterized by high accuracy and quadratic elements would be a better choice for more accurate results.

The proposed methodology, possibly improved with the employment of quadratic elements, can be used to perform parametric studies by varying the depth, length and width of the trench and by increasing the distance between the source and the trench to obtain effective amplitude reduction. One can also study the screening efficiency of multiple trenches. Thus useful design guidelines can be established for the benefit of the practicing engineer. In addition, the present methodology can be used to validate various experimental studies. These aspects will be the subject of a future publication.

Acknowledgments

The authors are grateful to the National Science Foundation for supporting this work under grant CEE 81-09723 to the University of Minnesota and to the University of Minnesota Supercomputer Institute for making its facilities available to them. Many thanks are also due to Dr. G. Meixel for his help with the computer graphics and to Mrs H. Alexandridis-Balis for her excellent typing of the manuscript.

References

Achenbach, J. D. (1973): Wave propagation in elastic solids. Amsterdam: North Holland

Ahmad, S.; Banerjee, P. K. (1988): Time domain transient elasto-dynamic analysis of 3-D solids by BEM. Int. J. Num. Meth. Engng. 26, 1709–1728

Ahmad, S.; Manolis, G. D. (1987): Dynamic analysis of 3-D structures by a transformed boundary element method. Comput. Mech. 2, 185–196
Apsel, R. J.; Luco, J. E. (1983): On the Green's functions for a layered half-space, Part II. Bull. Seism. Soc. Am. 73, 931–951
Banerjee, P. K.; Ahmad, S. (1985): Advanced three-dimensional dynamic analysis by boundary elements. In: Cruse, T. A.; Pifko, A. B.; Armen, H. (eds.): Advanced topics in boundary element analysis, AMD-Vol. 72, pp. 65–81, New York: ASME
Banerjee, P. K.; Ahmad, S.; Manolis, G. D. (1986): Transient elastodynamic analysis of three-dimensional problems by boundary element method. Earthquake Engng. Struct. Dyn. 14, 933–949
Banerjee, P. K.; Ahmad, S.; Manolis, G. D. (1987): Advanced elastodynamic analysis. In: Beskos, D. E. (ed.): Boundary element methods in mechanics. pp. 257–284. Amsterdam: North-Holland
Beskos, D. E. (1987): Boundary element methods in dynamic analysis, Appl. Mech. Rev. 40, 1–23
Beskos, D. E.; Dasgupta, B.; Vardoulakis, I. G. (1985): Vibration isolation of machine foundations. In: Gazetas, G.; Selig, E. T. (eds.): Vibration problems in geotechnical engineering, pp. 138–151. New York: ASCE
Beskos, D. E.; Dasgupta, B.; Vardoulakis, I. G. (1986): Vibration isolation using open or filled trenches. Part 1: 2-D homogeneous soil. Comput. Mech. 1, 43–63
Dasgupta, B. (1987): Vibration isolation of structures in a homogeneous elastic soil medium. Ph.D. Thesis. Minneapolis: University of Minnesota
Dasgupta, B.; Beskos, D. E.; Vardoulakis, I. G. (1986): 3-D Vibration isolation using open trenches. In: Shaw, R. P. et al. (eds.): Innovative numerical methods in engineering. pp. 385–392. Berlin, Heidelberg, New York: Springer
Dominguez, J. (1978a): Dynamic stiffness of rectangular foundations. Report R 78-20. Dept. of Civil Engng., Cambridge Mass: M.I.T.
Dominguez, J. (1978b): Response of embedded foundations to travelling waves. R 78-24, Dept. of Civil Engng., Cambridge Mass.: M.I.T.
Dominguez, J.; Abascal, R. (1987): Dynamics of foundations. In: Brebbia, C. A. (ed.): Topics in boundary element research. Vol. 4 applications in geomechanics. pp. 27–75, Berlin, Heidelberg, New York: Springer
Dominguez, J.; Alarcón, E. (1981): Elastodynamics. In: Brebbia, C. A. (ed.): Progress in boundary element methods—Vol. 1, pp. 213–257. London: Pentech Press
Eringen, A. C.; Suhubi, E. S. (1975): Elastodynamics. Vol. 2, Linear theory. New York: Academic Press
Gaitanaros, A. P.; Karabalis, D. L. (1986): 3-D flexible embedded machine foundations by BEM and FEM. In: Karabalis, D. L. (ed.): Recent applications in computational mechanics. pp. 81–96. New York: ASCE
Huh, Y.; Schmid, G. (1984): Application of boundary elements to soil-structure interaction problems. Engng. Anal. 1, 170–173
Jain, D. L.; Kanwal, R. P. (1978): Scattering of P and S waves by spherical inclusions and cavities. J. Sound Vibr. 57, 171–202
Karabalis, D. L.; Beskos, D. E. (1984): Dynamic response of 3-D rigid surface foundations by time domain boundary element method. Earthquake Engng. Struct. Dyn. 12, 73–93
Karabalis, D. L.; Beskos, D. E. (1985): Dynamic response of 3-D flexible foundations by time domain BEM and FEM. Soil Dyn. Earthquake Engng. 4, 91–101
Karabalis, D. L.; Beskos, D. E. (1986): Dynamic response of 3-D embedded foundations by the boundary element method. Comp. Meth. Appl. Mech. Engng. 56, 91–119
Karabalis, D. L.; Beskos, D. E. (1987a): Three-dimensional soil-structure interaction by boundary element methods. In: Brebbia, C. A. (ed.): Topics in boundary element research. Vol. 4, applications in geomechanics. pp. 1–26. Berlin, Heidelberg, New York: Springer
Karabalis, D. L.; Beskos, D. E. (1987b): Dynamic soil-structure interaction. In: Beskos, D. E. (ed.): Boundary element methods in mechanics. pp. 499–562. Amsterdam: North-Holland
Karabalis, D. L.; Mohammadi, M. (1986): The application of the boundary element method to dynamic soil-structure interaction problems: computational aspects. In: Ranson, W. F.; Biedenbach, J. M. (eds.): Proc. of the 13th southeastern conference on theoretical and applied mechanics. pp. 321–328. Columbia: University of South Carolina
Kitahara, M.; Koshimizu, M.; Nakagawa, K. (1987): Three dimensional elastodynamic inclusion analysis. In: Brebbia, C. A.; Wendland, W. L.; Kuhn, G. (eds.): Boundary elements IX, Vol. 3: fluid flow and potential applications. pp. 139–148. Berlin, Heidelberg, New York: Springer
Kitahara, M.; Nakagawa, K. (1985): Boundary integral equation methods in three dimensional elastodynamics. In: Brebbia, C. A.; Maier, G. (eds.): Boundary elements VII. pp. 6.27–6.36. Berlin, Heidelberg, New York: Springer
Knopoff, L. (1959a): Scattering of compression waves by spherical obstacles. Geophysics 24, 30–39
Knopoff, L. (1959b): Scattering of shear waves by spherical obstacles. Geophysics 24, 209–219
Kobayashi, S. (1987): Elastodynamics. In: Beskos, D. E. (ed.): Boundary element methods in mechanics. pp. 191–255. Amsterdam: North-Holland
Kobayashi, S.; Mori, K. (1986): Three-dimensional dynamic analysis of soil-structure interactions by boundary integral equation-finite element combined method. In: Shaw, R. P. et al. (eds.): Innovative numerical methods in engineering. pp. 613–618. Berlin, Heidelberg, New York: Springer
Kobayashi, S.; Nishimura, N. (1980): Green's tensors for elastic half-spaces—an application of boundary integral equation method. Memoirs Fac. Engng. Koyoto Univ. 42, 228–241
Kobayashi, S.; Nishimura, N.; Mori, K. (1986): Applications of boundary element–finite element combined method of three-dimensional viscoelastodynamic problems. In: Qinghua Du (ed.): Boundary elements. pp. 67–74. Oxford: Pergamon Press
Lee, V. W. (1982): A note on the scattering of elastic plane waves by a hemispherical canyon. Soil Dyn. Earthquake Engng. 1, 122–129
Lee, V. W.; Trifunac, M. D. (1982): Body wave excitation of embedded hemisphere. J. Engng. Mech. Div. ASCE 108, 546–563
Luco, J. E.; Apsel, R. J. (1983): On the Green's functions for a layered half-space. Part I. Bull. Seism. Soc. Am. 73, 909–929
Manolis, G. D. (1984): Boundary element method for soil-structure interaction. In: Beskos, D. E.; Krauthammer, T.; Vardoulakis, I. (eds.): Dynamic soil-structure interaction, pp. 85–91. Rotterdam: Balkema

Manolis, G. D.; Beskos, D. E. (1988): Boundary element methods in elastodynamics. London: Unwin Hyman
Mohammadi, M.; Karabalis, D. L. (1986): Dynamic soil-structure interaction by the boundary element method: a comparative study. In: Will, K. M. (ed.): Electronic computation. pp. 220–231. New York: ASCE
Nakagawa, K.; Kitahara, M. (1986): Transient analysis in three-dimensional elastodynamics. Show, R. P. et al. (eds.): Innovative numerical methods in engineering. pp. 367–377. Berlin, Heidelberg, New York: Springer
Niwa, Y.; Hirose, S. (1985): Three-dimensional analysis of ground motion by integral equation method in wave number domain. In: Kawamoto, T.; Ichikawa, Y. (eds.): Numerical methods in geomechanics Nagoya 1985. pp. 143–149. Rotterdam: Balkema
Niwa, Y.; Hirose, S. (1986): Application of the BEM to elastodynamics is a three-dimensional half-space. In: Karabalis, D. L. (ed.): Recent applications in computational mechanics. pp. 1–15. New York: ASCE
Ottenstreuer, M. (1982): Frequency dependent dynamic response of footings. In: Cakmak, A. S., Abdel-Ghaffar, A. M.; Brebbia, C. A. (eds.): Soil dynamics and earthquake engineering. pp. 799–809. Rotterdam: Balkema
Ottenstreuer, M.; Schmid, G. (1981): Boundary elements applied to soil-foundation interaction. In: Brebbia, C. A. (ed.): Boundary element methods. pp. 293–309. Berlin, Heidelberg, New York: Springer
Pao, Y. H.; Mow, C. C. (1963): Scattering of plane compressional waves by a spherical obstacle. J. Appl. Phys. 34, 493–499
Pao, Y. H.; Mow, C. C. (1971): Diffraction of elastic waves and dynamic stress concentrations. New York: Crane Russak
Richart, Jr., F. E.; Hall, Jr., J. R.; Woods, R. D. (1970): Vibrations of soils and foundations. Englewood Cliffs, N. J.: Prentice Hall
Rizzo, F. J.; Shippy, D. J.; Rezayat, M. (1985a): Boundary integral equation analysis for a class of earth-structure interaction problems. Report to NSF CEE-8013461. Department of Engineering Mechanics, Lexington: University of Kentucky
Rizzo, F. J.; Shippy, D. J.; Rezayat, M. (1985b): A boundary integral equation method for radiation and scattering of elastic waves in three dimensions. Int. J. Num. Meth. Engng. 21, 115–129
Rizzo, F. J.; Shippy, D. J.; Rezayat, M. (1985c): A boundary integral equation method for time-harmonic radiation and scattering in an elastic half-space. In: Cruse, T. A.; Pifko, A. B.; Armen, H. (eds.): Advanced topics in boundary element analysis, AMD-Vol. 72. pp. 83–89. New York: ASME
Rezayat, M.; Shippy, D. J.; Rizzo, F. J. (1986): On time-harmonic elastic-wave analysis by the boundary element method for moderate to high frequencies. Comp. Meth. Appl. Mech. Engng. 55, 349–367
Sánchez-Sesma, F. J. (1983): Diffraction of elastic waves by three-dimensional surface irregularities. Bull. Seism. Soc. Amer. 73, 1621–1636
Tassoulas, J. L. (1989): Dynamic soil-structure interaction In: Beskos, D. E. (ed.): Boundary element methods in structural analysis, pp. 273–308, New York: ASCE
Wong, H. L.; Luco, J. E. (1976): Dyanmic response of rigid foundations of arbitrary shape. Earthquake Engng. Struct. Dyn. 4, 579–587

Communicated by S. N. Atluri, January 4, 1989